

# Denoising of ABR Signals using Wavelet Packets

Nivin Ghamry

Department of Information Technology  
Faculty of Computer and Information, Cairo, Egypt  
Email: nivin {at} fci-cu.edu.eg

**Abstract**—Auditory Brainstem Response (ABR) is an auditory evoked potential extracted from ongoing electrical activity in the brain. ABR is especially used for newborn- and children hearing screening, auditory threshold estimation, and brainstem lesion detection in response to stimuli such as click sound, tone burst or chirp. In order to support clinical decision making the analysis of ABR signals must exhibit good resolution in both time domain and frequency domain. In this paper biorthogonal wavelet packets are applied for effective noise reduction and detection of ABR signals. Experimental results obtained of simulated data run on Matlab and real data demonstrate the superiority of wavelet packets for denoising and reconstructing ABR signals.

**Keywords**- auditory brainstem response, biorthogonal wavelet packets, denoising.

## I. INTRODUCTION

Most of the statistical characteristics of biomedical signals are non-stationary. The application of Discrete Wavelet Transform (DWT) as a general mathematical tool for processing of nonstationary biomedical signals includes filtering out redundancies from measured signals, signal decomposition and data compression preserving signal quality. Another application of DWT is feature detection, which is required for clinical diagnosis of signals [1]. In [2], [3] and [4] wavelets have been used to filter and analyze noisy electrocardiogram (ECG) signals as well as to detect the positions of occurrence of the QRS complex during the period of analysis. QRS complex is a name for the combination of three of the graphical deflections seen on a typical ECG. In [5] a scheme based on Generalized Fractal Dimensions GFD and DWT analysis of electroencephalogram (EEG) signals was developed. Fast Fourier Transform (FFT) and wavelet transform have been used by researchers in neurologic tests like Auditory Brainstem Response (ABR) for detection of hearing loss [6]. In [7] the continuous wavelet transform (CWT) of ABR signal had been introduced as a marker to identify the ABR waves. Feature Extraction and Classification of the ABR using wavelet analysis is illustrated in [8]. ABR signals are usually contaminated with noise because of interference and other brain activities in ABR signal. This noise must be removed from the data in order to proceed with further data analysis. One of the most important applications of wavelets is in removal of noise from signals, or denoising, accomplished by thresholding wavelet coefficients to separate signal from noise. Research work in this area has been summed in [9]. In [10] a signal-adaptive denoising technique

based on complex wavelets is proposed to optimally denoise ABR signals and perform reliable waveform analysis. In the current work biorthogonal wavelet packets are applied for effective noise reduction and retrieving the underlying wave V of ABR signals. The signal is decomposed into individual scales to create different frequency bands with different features of the original signal. Thresholding technique is applied for denoising, then the ABR signal is reconstructed at wavelet from approximation and detail scales. The proposed method has been tested on normal and impaired adult subjects. The ABR signal is collected using high accuracy bio signal data acquisition and processing system. Experimental results with simulated data run on Matlab and real data demonstrate the superiority of wavelet packets for the denoising and reconstructing ABR data.

This paper is organized as follows, in section II ABR signal are briefly introduced and explained. In section III biorthogonal wavelet packet transform is reviewed and its application for multi-resolution analysis for AEP signals is described. The proposed method for multi-resolution analysis is described in section IV. Experimental results obtained with simulated data run on Matlab and real data are demonstrated are given in section V and finally conclusions are given in section VI.

## II. AUDITORY BRAINSTEM RESPONSE (ABR)

The Auditory Brainstem Response (ABR) is one of the most widely used auditory evoked potentials (AEP) as well as one of the best recognized electrophysiological tools used by audiologists. It is used for neurodiagnostic purposes to detect lesions on the eighth nerve and brainstem as well as for threshold testing. The ABR is an electrophysiologically recorded signal in EEG which represents the summed and differentially averaged responses of thousands of nerve fibers to repeated acoustic stimulation. It is generated by a brief click or tone pip transmitted from an acoustic transducer in the form of an insert earphone or headphone. The signal consists of very low amplitude signal (in range of a few nano Volts) extracted from ongoing electrical activity in the brain and recorded via surface electrodes placed at the vertex of the scalp and ear lobes. These signals typically have a signal-to-noise ratio (SNR) well below 10 dB [11]. The resulting recording is a series of vertex positive waves of which I through V are evaluated [12]. These waves, labeled with Roman numerals in Jewett and Williston convention, occur in the first 10 milliseconds after onset of an auditory stimulus

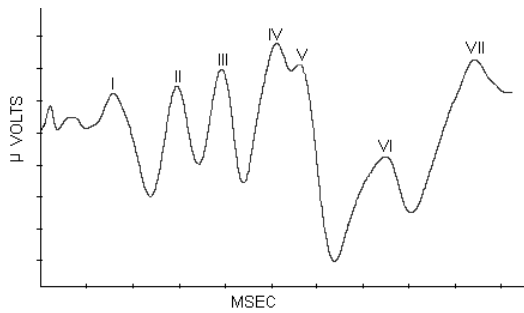


Figure1. A typical ABR with normal auditory function.

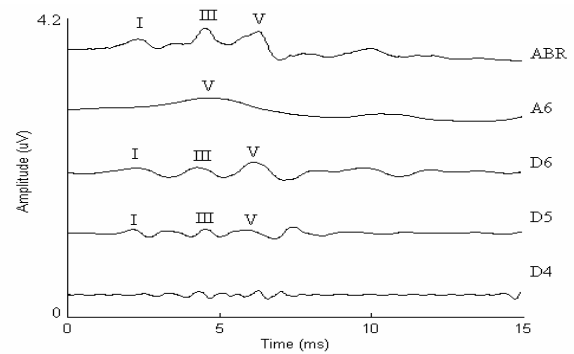


Figure2. ABR signal and its reconstructed DWT signals.

presented at high intensities in the range of 70-90 dB normal hearing level (nHL).

The auditory structures that generate the auditory brainstem response are as follows:

- Wave I – generated by cranial nerve VIII
- Wave II – generated by the cochlear nucleus
- Wave III – generated by the superior olivary complex
- Wave IV – generated by the lateral lemniscus
- Wave V – generated by the inferior colliculus

A typical ABR from an adult with normal auditory function is shown in Figure 1. When interpreting the ABR the following parameters are considered:

- amplitude, which is the number of neurons firing,
- latency, which is the speed of transmission,
- interpeak latency, which is the time between peaks,
- interaural latency which is the difference in wave V latency between ears.

The ABR represents initiated activity beginning at the base of the cochlea and moving toward the apex over a 4ms period of time. The peaks largely reflect activity from the most basal regions on the cochlea because the disturbance hits the basal end first and by the time it gets to the apex, a significant amount of phase cancellation occurs. There are five categories of response based on their occurrence after the stimulation [13].

- Fast responses occur between 2 and 12 msec.
- SWR responses (slow wave components of the brainstem) occur after 12 msec.
- Middle responses occur between 12 and 50 msec.
- Slow responses occur between 50 and 300 msec.
- Late responses occur 250 to 600 msec after stimulation.

### III. MULTI-RESOLUTION ANALYSIS FOR AEP SIGNALS USING WPT

Multi-resolution detection methods have been initially proposed to detect peaks of ABR signals using a narrow-band filters, and then obtain a more accurate estimate of peak latency using a broader band-pass filter, as illustrated in [14]. This coarse-to-fine strategy improves detection at low stimulus intensities as the narrow-band filter has an improved signal-to-noise ratio (SNR), whilst the broader band filter has

improved temporal resolution. Because of its MRA capability, the DWT has been a valuable tool for the analysis of transient signals like electrophysiological potentials. The orthogonal basis functions produced by the DWT provide good spectral localization at low frequency and good temporal resolution at high frequency [15]. Projection of an input signal on these basis functions provides simultaneous access to time, amplitude, and scale (frequency) information, and therefore the ability to conduct efficient MRA. Furthermore, the DWT is now being widely applied to the MRA of AEP. A typical MRA of AEP includes decomposing the signal into individual scales to create different frequency bands including different features of the original signal. Figure 2 shows a reconstructed ABR signal from DWT coefficients at wavelet approximation scale A6, and detail scales D6, D5 and D4 using the Daubechies mother wavelet (db5)[16]. As shown in figure, A6 is the low frequency component of peak V, while D6 and D5 and D4 are the medium and high frequency components of peaks I, III, and V respectively. In the following part biorthogonal wavelet packets applied in this work are reviewed briefly.

#### A. Biorthogonal Wavelet versus Daubechies Wavelets

Since the application of wavelet transformation in electrocardiology is relatively new, choosing the best mother wavelet for AEP MRA is a big challenge to improve the clinical use of it especially as many wavelet properties cannot be jointly optimized. Although the Daubechies mother wavelets (dbn) have minimum support length for a given number of vanishing moments, they are not optimal in the sense of symmetry and smoothness. Biorthogonal wavelets provide symmetry (linear phase) and smoothness (regularity). Linear phase is generally a desirable property of digital filters as it means that a number of in-phase frequency components pass through a linear phase filter and will be in-phase at the output, which avoids phase distortion [15]. For MRA of time varying AEP signals, using mother wavelets with a linear phase is critical because of the following reasons:

- morphology and latency of peaks as well as all filtering operations must preserve phase.
- The location and amplitude of peaks is highly dependent upon the relative phase of the frequency components in the signal.

Therefore it is important to select a smooth wavelet with minimal support length.

**B. Biorthogonal Wavelet Packets**

More flexible time-frequency localization is obtained by wavelet packet transform. Wavelet packet transform was first introduced by Coifman et al [17] for dealing with the nonstationarities of the data. It has been applied as an efficient signal processing methods for MRA and local feature extraction of nonstationary signals. Fig 3 shows the basic structure of WPT, where  $h(n)$  and  $g(n)$  are the low- and high pass filters, respectively. In difference to the DWT, the signal is iterated over all frequency bands at each level, which leads to a full tree decomposition. The best-tree searching algorithm is then applied to decide a subset of the full tree as the final decomposition structure by measuring a data dependent cost function. Commonly used cost functions in the field of signal processing are entropy types. Denoising of signals using WPT was first developed by Donoho and Johnstone[18] based on thresholding after signal decomposition to a certain level. Types of thresholding are hard and soft thresholding. The soft thresholding involves first setting to zero the elements whose absolute values are lower than the threshold, and then shrinking the nonzero coefficients towards zero. Denoising of the coefficients is achieved via soft thresholding given by Equation (1):

$$T_j = \sigma_j \sqrt{2 \ln N / 2^j} \quad (1)$$

Where  $N$  is the length of the input signal and  $\sigma$  is the standard deviation of noise at scale  $j$ .  $T_j$  is the threshold calculated on a level-dependent basis.

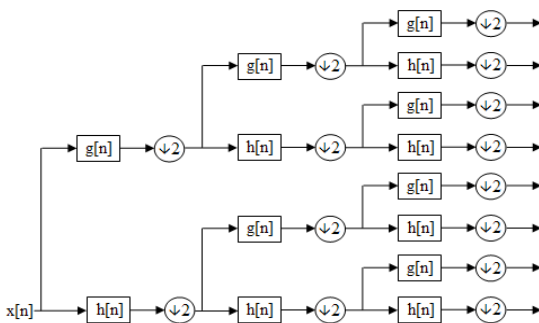


Figure3. The architecture of the wavelet packet transform

**IV. METHOD AND EQUIPMENT**

**A. Equipment and Setup**

In the following the equipment used to detect and record auditory brainstem response with the MP data acquisition system are listed [19]:

- MP acquisition system (MP100 or MP150)
- Evoked response amplifier module (ERS100A)

- Stimulator module (STM100A)
- Tubephone (OUT101)
- 3 x disposable electrodes (EL503)
- Unshielded lead (LEAD110)
- 2 x Shielded leads (LEAD110S)

For hardware setup, the MP unit is connected to the computer, the STM100C module is connected to the UIM100C and the MP unit. The ERS100C is connected to the free side of the UIM100 modem driver. The ERS100C module and STM100C module are set. The scale of the channel it to read in "µVolts" and the number of averages is set to 2000. The type of stimuli used is clicks.

**B. Method**

Differentially averaged Brainstem Response testing is used. As the amplitude of the ABR is quite small compared to the "noise" component of the EEG, the signal to noise ratio is enhanced by averaging. In this study, it was focused on the presence and peak detection of wave V. As wave V has the largest amplitude at or near threshold it is considered to be the most significant and the waveform most likely to be reliably present. Several real ABR signal from normal subjects and subjects with hearing loss are recorded. The raw ABR signals taken from the Bio-logic EVP system in ASCII format and transferred to a personal computer running Mathworks Matlab. Six-level WPT decompositions with biorthogonal spline wavelet B5 are performed on each ABR signal. For each wavelet decomposition level (except for the approximation coefficients), a level dependent soft threshold is determined. Soft thresholding is applied on the wavelet coefficients to kill or reduce the effect of the noise. Figure 4 shows biorthogonal B-spline mother wavelets used in this work.

**V. RESULTS AND DISCUSSIONS**

Figure 4 shows the reconstructed normal ABR waveforms of left and right ear. Considering Wave V, it can be seen that various high level contours still appeared, while the hearing level(HL) is reduced for 80dB to 30dB for both ears. Waveform details, as normal hearing level nHL, rate of stimulation, type of stimulus (clicks), amplification gain(100K) and frequency (100Hz) are given in Table 1(a).

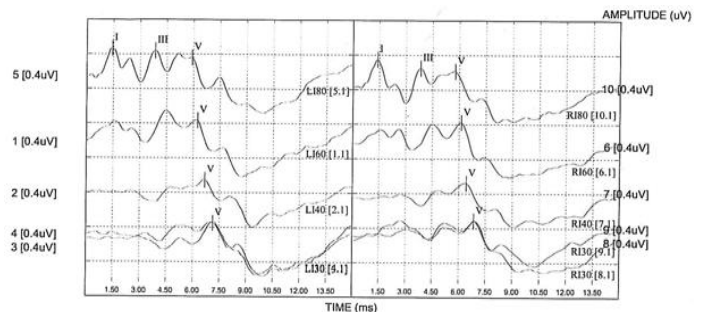


Figure 4. Reconstructed normal ABR waveforms of left and right ear.

TABLE 1 EVOKED POTENTIAL REPORT FOR NORMAL HEARING

WAVEFORMS															
ABR															
#	Date	Transducer	nHL	Ear	Rate	Stimulus	Gain	High	Low	Acc	Rej	Epoch	Time/div	Delay	
1	4/30/2014	1.1	Insert Phone	60 dB	Left	21.1/s	Click-R	100K	100 Hz	3 kHz	927	0	15ms	1.50ms	0.0ms
2	4/30/2014	2.1	Insert Phone	40 dB	Left	21.1/s	Click-R	100K	100 Hz	3 kHz	781	0	15ms	1.50ms	0.0ms
3	4/30/2014	3.1	Insert Phone	30 dB	Left	21.1/s	Click-R	100K	100 Hz	3 kHz	732	0	15ms	1.50ms	0.0ms
4	4/30/2014	4.1	Insert Phone	30 dB	Left	21.1/s	Click-R	100K	100 Hz	3 kHz	812	0	15ms	1.50ms	0.0ms
5	4/30/2014	5.1	Insert Phone	80 dB	Left	21.1/s	Click-R	100K	100 Hz	3 kHz	775	0	15ms	1.50ms	0.0ms
6	4/30/2014	6.1	Insert Phone	60 dB	Right	21.1/s	Click-R	100K	100 Hz	3 kHz	847	0	15ms	1.50ms	0.0ms
7	4/30/2014	7.1	Insert Phone	40 dB	Right	21.1/s	Click-R	100K	100 Hz	3 kHz	949	0	15ms	1.50ms	0.0ms
8	4/30/2014	8.1	Insert Phone	30 dB	Right	21.1/s	Click-R	100K	100 Hz	3 kHz	909	0	15ms	1.50ms	0.0ms
9	4/30/2014	9.1	Insert Phone	30 dB	Right	21.1/s	Click-R	100K	100 Hz	3 kHz	1001	9	15ms	1.50ms	0.0ms
10	4/30/2014	10.1	Insert Phone	80 dB	Right	21.1/s	Click-R	100K	100 Hz	3 kHz	818	0	15ms	1.50ms	0.0ms

(a)

LATENCIES (ms)						
ABR						
Waveform	Ear	I	II	III	IV	VI
1	Left	***	***	***	***	6.25
2	Left	***	***	***	***	5.66
4	Left	***	***	***	***	7.13
5	Left	1.45	***	3.85	***	5.33
6	Right	***	***	***	***	6.13
7	Right	***	***	***	***	6.43
9	Right	***	***	***	***	6.85
10	Right	1.60	***	3.83	***	5.78

(b)

In Table 1(b) the number of waveforms in which wave V is recognizable and the corresponding latencies are listed. For the left ear the latencies of waveforms 1, 2, 4, 5 are listed and for right ear the latencies of waveforms 6, 7, 9, 10 are listed. The latency increases as the nHL is decreased, for example, in waveform 4 and 9. Figure 5 shows abnormal ABR waveforms. It can be clearly seen that the contour levels of wave V are mostly not recognizable starting nHL of 50dB for both ears. Waveform details are given in Table 2(a). In Table 2(b) the latencies of waveforms 1, 2, 8 for the left ear are listed and for right ear the latencies of waveforms 3, 7, 9 are listed.

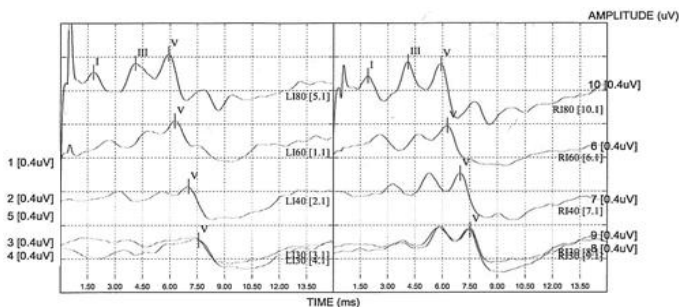


Figure 5. Reconstructed abnormal ABR waveforms of left and right ear

TABLE 2 EVOKED POTENTIAL REPORT FOR ABNORMAL HEARING

WAVEFORMS															
ABR															
#	Date	Transducer	nHL	Ear	Rate	Stimulus	Gain	High	Low	Acc	Rej	Epoch	Time/div	Delay	
1	4/30/2014	1.1	Insert Phone	60 dB	Left	21.1/s	Click-R	100K	100 Hz	3 kHz	927	0	15ms	1.50ms	0.0ms
2	4/30/2014	2.1	Insert Phone	40 dB	Left	21.1/s	Click-R	100K	100 Hz	3 kHz	781	0	15ms	1.50ms	0.0ms
3	4/30/2014	3.1	Insert Phone	30 dB	Left	21.1/s	Click-R	100K	100 Hz	3 kHz	732	0	15ms	1.50ms	0.0ms
4	4/30/2014	4.1	Insert Phone	30 dB	Left	21.1/s	Click-R	100K	100 Hz	3 kHz	812	0	15ms	1.50ms	0.0ms
5	4/30/2014	5.1	Insert Phone	80 dB	Left	21.1/s	Click-R	100K	100 Hz	3 kHz	775	0	15ms	1.50ms	0.0ms
6	4/30/2014	6.1	Insert Phone	60 dB	Right	21.1/s	Click-R	100K	100 Hz	3 kHz	847	0	15ms	1.50ms	0.0ms
7	4/30/2014	7.1	Insert Phone	40 dB	Right	21.1/s	Click-R	100K	100 Hz	3 kHz	949	0	15ms	1.50ms	0.0ms
8	4/30/2014	8.1	Insert Phone	30 dB	Right	21.1/s	Click-R	100K	100 Hz	3 kHz	909	0	15ms	1.50ms	0.0ms
9	4/30/2014	9.1	Insert Phone	30 dB	Right	21.1/s	Click-R	100K	100 Hz	3 kHz	1001	9	15ms	1.50ms	0.0ms
10	4/30/2014	10.1	Insert Phone	80 dB	Right	21.1/s	Click-R	100K	100 Hz	3 kHz	818	0	15ms	1.50ms	0.0ms

(a)

LATENCIES (ms)						
ABR						
Waveform	Ear	I	II	III	IV	VI
1	Left	1.95	***	3.63	***	5.30
2	Left	***	***	***	***	5.90
3	Right	1.68	***	3.63	***	5.25
7	Right	2.08	***	3.63	***	5.35
8	Left	1.83	***	3.55	***	5.10
9	Right	***	***	***	***	6.08

(b)

An illustration of severe hearing loss is given in Figure, which shows that that the contours almost disappeared starting HL of 60dB for the left ear and 80dB for right compared with normal signal, which contains various levels of contours. Waveform details are given in Table 3(a). In Table 3(b) the latencies of waveforms 2, 3, 5 for the left ear are listed and for right ear the latency of only waveform 11 is given

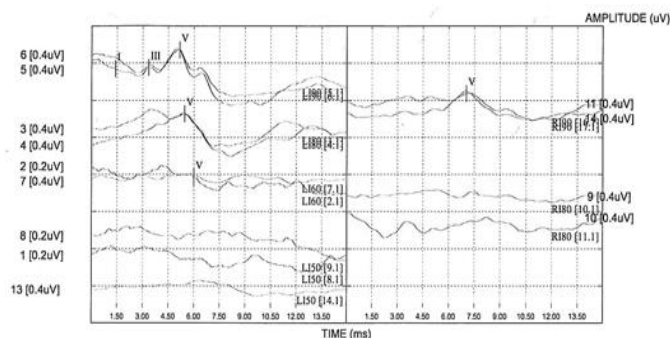


Figure 7. ABR waveforms of left and right ear for severe hearing loss.

TABLE 3 EVOKED POTENTIAL REPORT FOR SEVERE HEARING LOSS

WAVEFORMS															
ABR															
#	Date	Transducer	nHL	Ear	Rate	Stimulus	Gain	High	Low	Acc	Rej	Epoch	Time/div	Delay	
1	3/10/2014	8.1	Insert Phone	50 dB	Left	21.1/s	Click-R	100K	100 Hz	3 kHz	1235	0	15ms	1.50ms	0.0ms
2	3/10/2014	2.1	Insert Phone	60 dB	Left	21.1/s	Click-R	100K	100 Hz	3 kHz	1293	0	15ms	1.50ms	0.0ms
3	3/10/2014	3.1	Insert Phone	80 dB	Left	21.1/s	Click-R	100K	100 Hz	3 kHz	1225	0	15ms	1.50ms	0.0ms
4	3/10/2014	4.1	Insert Phone	80 dB	Left	21.1/s	Click-R	100K	100 Hz	3 kHz	1221	0	15ms	1.50ms	0.0ms
5	3/10/2014	5.1	Insert Phone	90 dB	Left	21.1/s	Click-R	100K	100 Hz	3 kHz	1215	0	15ms	1.50ms	0.0ms
6	3/10/2014	6.1	Insert Phone	80 dB	Left	21.1/s	Click-R	100K	100 Hz	3 kHz	2000	0	15ms	1.50ms	0.0ms
7	3/10/2014	7.1	Insert Phone	50 dB	Left	21.1/s	Click-R	100K	100 Hz	3 kHz	1705	0	15ms	1.50ms	0.0ms
8	3/10/2014	8.1	Insert Phone	80 dB	Right	21.1/s	Click-R	100K	100 Hz	3 kHz	1121	0	15ms	1.50ms	0.0ms
9	3/10/2014	9.1	Insert Phone	80 dB	Right	21.1/s	Click-R	100K	100 Hz	3 kHz	1028	0	15ms	1.50ms	0.0ms
10	3/10/2014	10.1	Insert Phone	90 dB	Right	21.1/s	Click-R	100K	100 Hz	3 kHz	1181	0	15ms	1.50ms	0.0ms
11	3/10/2014	14.1	Insert Phone	80 dB	Left	21.1/s	Click-R	100K	100 Hz	3 kHz	1921	0	15ms	1.50ms	0.0ms
13	3/10/2014	14.1	Insert Phone	90 dB	Left	21.1/s	Click-R	100K	100 Hz	3 kHz	1357	0	15ms	1.50ms	0.0ms

(a)

LATENCIES (ms)						
ABR						
Waveform	Ear	I	II	III	IV	VI
2	Left	***	***	***	***	6.00
3	Left	***	***	***	***	5.45
5	Left	1.40	***	3.35	***	5.15
11	Right	***	***	***	***	7.03

(b)

## VI. COCLUSION

In this paper B-spline biorthogonal wavelet packets have been successfully exploited for detection of ABR signals. This could be achieved as linear phase and symmetry met by the bi-orthogonal spline wavelets are critical features for AEP multiresolution analysis. Simulation results obtained of real data have shown that the symmetry of the biorthogonal wavelet avoids phase distortion and the regularity provides smoothness of the reconstructed waveforms. Furthermore, it has been demonstrated that the denoising property of wavelet packets produces accurate estimates of peak amplitudes of wave V and latencies present in EVP reports of normal and abnormal hearing cases.

## ACKNOWLEDGMENT

The author acknowledges the technical and medical support of Dr Ghada Abo Elhadid, lecturer of audiology in Aladan Hospital of Kuwait, during all phases of work.

## REFERENCES

- [1] G. Kaushik, H.P.Sinha, "Biomedical signal analysis through wavelets: A review," International Journal of Advanced Research in Computer Science and Software Engineering, volume 2, issue 9, pp.422-428 September 2012.
- [2] S.Sumathi and M.Y. Sanavullah, "Comparative study of QRS complex detection in ECG Based on Discrete Wavelet Transform," International Journal of Recent Trends in Engineering, vol. 2, no. 5, pp. 273–277, November 2009.
- [3] H.M. Rai and A. Trivedi, "De-noising of ECG Waveforms based on Multi-resolution Wavelet Transform", International Journal of Computer Applications, vol. 45, no.18, May 2012.
- [4] P. Karthikeyan, M. Murugappan, and S.Yaacob, "ECG Signal denoising using wavelet thresholding techniques in human stress assessment", International Journal on Electrical Engineering and Informatics, vol. 4, no. 2, 2012.
- [5] D. Easwaramoorthy and R. Uthayakumar, "Analysis of biomedical EEG signals using wavelet transforms and multifractal analysis," IEEE International Conference on Communication Control and Computing Technologies (ICCCCT), pp. 544 – 549, October 2010.
- [6] W. J. Wilson, and F. Aghdasi, "Fast Fourier Transform analysis of the auditory brainstem response: Effects of stimulus intensity and subject age, gender and test ear," *AFRICON IEEE*, vol. 1, pp. 285- 290, 1999.
- [7] M. M. Rushaidin, Sh.-Hussain Salleh, O. Hazi, H. Mahyar, C. M. Ting, and A. K. Ari, "Wave V detection using continuous wavelet transform of auditory brainstem response signal", Proceedings of Progress in electromagnetics research symposium, pp. 1889-1893, March 2012, Malaysia.
- [8] R. Zhang, G. Mc Allister, "Feature extraction and classification of the auditory brainstem response using wavelet analysis", Knowledge Exploration in Life Science Informatics, Lecture Notes in Computer Science, vol. 3303, pp. 169-180, 2004.
- [9] Li Yuenan, S. Ying, "Research on wavelet de-noising method of auditory brainstem response", Chinese Journal of Scientific Instrument, 2010
- [10] A. Jacquin, E. Causevic, E. R. John and L. S. Pritchep, "Optimal denoising of brainstem Auditory Evoked Response (BAER) for automatic peak identification and brainstem assessment.," Conf Proc IEEE Eng Med Biol Soc, 2006, vol. 1, pp.1723-1726.
- [11] A.Macy The Handbook of Human Physiological Recording, Chapter 7: Stimulus and Response, Jaypee Brothers Medical Publishers, 1993.
- [12] N. Bhattacharyya, "Auditory Brainstem Response Audiometry", Medscape, March 2013.
- [13] J. Hall, Handbook of auditory evoked responses, Needham Heights, Massachusetts: Allyn and Bacon, 1992.
- [14] H. Pratt, D.Urbach, and N. Bleich, "Auditory brainstem evoked potentials peak identification by finite impulse response digital filters," Audiology, vol. 28, pp. 272-283, 1989.
- [15] Mallat, S.G., A Wavelet tour of signal processing, 2nd Ed., San Diego: Academic Press, 1999.
- [16] A. Bradley, W.J. Wilson, On wavelet analysis of auditory evoked potentials, Official Journal of the International Federation of Clinical Neurophysiology, vol. 115, pp. 1114-1128, 2004.
- [17] R.R.; Coifman, M.V Wickerhauser, Signal processing and compression with wave packets, Numerical Algorithms Research Group, New Haven, CT Yale University, 1990.
- [18] D. L. Donoho, and I.M. Johnstone, Ideal spatial adaptation via wavelet shrinkage, Biometrika 81, pp. 425-455, 1994.
- [19] Auditory brainstem response testing, BIOPAC Systems, Inc.